ALTERNATIVE PROBLEM FORMULATIONS FOR IDENTIFICATION OF MATHEMATICAL MODEL OF HELICOPTER ROTOR BLADE AND SOME PROBLEMS OF AEROELASTICITY ANALYSIS

Vadim Yu.Eremin, Ph.D, [1] Sergei E.Paryshev, Ph.D.[2]

[1,2] Central Aerohydrodynamic Institute n. a. prof. N.Ye. Zhukovsky (TsAGI)
Russia
sergei.paryshev@tsagi.ru

Keywords: blade, helicopter rotor, flutter, Campbell's diagramm, elastic modes, aeroelasticity, aerodynamic analysis, aerodynamic singularities, design process

Abstract: The task to provide multi-disciplinary engineering analysis of helicopter rotor blade is stated, as the most vital, in authors' opinion, to provide efficiency of the design process, where it is just the efficiency rather than deep insight into any of the discipline that has to be preferred.

Two contributing problems are considered within this task formulation:

- A combined analytical/experimental method to get Campbell's diagram for a helicopter blade has been developed. The method is based on experimental measurement of elastic compliance matrix of the blade at zero rotation speed. Results for actual blades are presented.

The vital demand of the task of blade characteristics identification goes from the fact that to get Campbell's diagram and vibration mode shapes of a rotating blade from appropriate dynamic response processing is rather a complicated problem; also any hardware to excite the blade under rotation may affect properties of the mechanical system and thus deteriorate the results.

- A problem of computational analysis of blade motion within the rotor is formulated, for which dynamic condensation approach is NOT used. For aerodynamic analysis, a discrete singularities method is used that makes it possible to calculate chord-wise aerodynamic forces exactly.

Also under discussion is the use of undeservedly forgotten abstract concepts like "suction force" and "chordwise variable inductive wash" closely associated with the theory of thin lifting surface.

1 INTRODUCTION

TsAGI's and world-wide experience of successful and unsuccessful developments in the area of multidisciplinary design of helicopter rotor blade [1] makes it possible to select efficient, not too complicated and proven computational techniques and to take into account most of the physical effects related to the problem.

A model of thin lifting surface is used for aerodynamic calculations. The effect of surface thickness on airfoil moment characteristics and lift curve slope is taken into account by

1

distribution of sources over the surface. Though simple, this approach provides very good results just competitive with panel methods. Comparison between the almost exact solution (by Christoffel-Shwartz integral) and thin lifting surface method for a thick 19% GU airfoil is presented below.

It should be noted that the Prandtl-Glauert transformation cannot be used to consider air compressibility as the equation for flow potential has variable coefficients if written in the system of coordinates connected to the blade. Thus an ordinary 4-dimensions wave equation has to be solved for a quasi-steady problem (4th coordinate is time). This problem is solved by the method of "descending along the coordinate (time)". Functions of influence of singularities (sources and vortices) moving along a helix line are used.

Basically, the above aerodynamic problem formulation allows us to formulate also the problem of noise propagation from the rotor due to blade lift force variations caused by blade elastic vibrations while flow is not separated. The problem of noise analysis due to boundary layer and due to flow separation is not stated.

In-house mech generator and settings module to set up finite elements properties and materials reology data has been made for NASTRAN'a. It accelerates data preparation for FE analysis. Once the blade geometry is set up or obtained from aerodynamic optimization module, then all the are is done automatically and faster than by use of PATRAN. Also automated are transferring aerodynamic loads onto FEM of the blade and generation of a matrix of aerodynamic influence coefficients (for static aeroelasticity analysis), matrices of aerodynamic stiffness and aerodynamic damping (for aeroelastic stability analysis).

Nonlinear formulation slightly complicates flutter analysis and makes programs running slower, which is undesirable for CAD/CAE software.

To accelerate program run time, a dedicated optimal algorithm has been developed for NASTRAN, which essentially shorten processor time for nonlinear analysis.

A cost effective procedure of identification of an elastic system well described by beam bending equations in the field of centrifugal inertial forces has been developed. This is equivalent to obtaining Campbell's diagram and vibration eigenmode shapes of a rotating blade. The key idea is the refusal from finding bending stiffness of the beam in a set of spanwise stations, but getting its flexibility matrix (structural influence coefficients) instead.

The above approaches are intended for use in blade flutter analysis. Appropriate software codes have been developed enabling fast calculation of multiple design configurations. Alongside with in-house programs, other well-proven developments, especially NASTRAN have been adapted for these problems.

2 THE AERODYNAMIC MODEL AND BRIEF COMPARISON WITH OTHER MODELS

A model of thin lifting surface is used for aerodynamic calculations. The effect of surface thickness on airfoil moment characteristics and lift curve slope is taken into account by distribution of sources over the surface. Though simple, this approach provides very good results just competitive with panel methods. Comparison between the almost exact solution (by Christoffel-Shwartz integral) and thin lifting surface method for a thick 19% GU airfoil is presented below.

Airfoil data	Christoffel-Shwartz integral	Thin lifting surface
C_{L0}	0.7921	0.7518
C_L^{α}	0.1275	0.1285
$C_{m(0.25)}$ at $\alpha=0$	-0.157	-0.158

Table 1: Airfoil data comparison

Of course the comparison is better for thinner surfaces

The thin lifting surface model allows pressure distribution to be calculated on both the surface sides with account for its thickness. The solutions are known to have integrable singularities at the edges free of trailing vortex sheet. A correction is used to get continuous pressure distribution. The correction is made by "transferring" flow potential from the thin lifting surface onto real blade surface, then flow velocity is calculated by differentiating along the surface. The correction does not change spanwise distribution of the circulation. The method enables consideration of viscous effect as the "external solution" is fairly smooth. The problem of airfoil shape design for assigned pressure distribution is also simple within this formulation, as well as other problems like airfoil modification to avoid "root effect on a sweptback wing", effect of sudden change of sweep angle, e.t.c.

A theoretical abstraction of "suction force" is associated with thin lifting surface theory. It is used to consider the fact that lifting force is not perpendicular to a lifting surface. The numerical techniques proposed by the authors allows for exact calculation of suction force on the edges, which is important for analysis of chord-wise loading and "chordwise flutter". Panel-based methods, especially Galerkin-based programs do not provide exact calculation of in-plane (chordwise) loading. Meanwhile, the authors are aware of the drawbacks of the thin surface method. Indicating drawbacks of other approaches, we just emphasize advantages of the thin surface method, but do not consider it as a universal one.

A theoretical abstraction of a chord-wise variable inductive wash-down is less known. It has been proven that chord-wise local distributed circulation within the blade aerodynamic system can be obtained from the solution of a two-dimensional problem of flow about an airfoil with taking into account an **inductive wash-down that is variable in chordwise direction**. It is rather similar to a theoretical abstraction of an inductive washdown that is constant in chordwise direction in the lifting vortex line theory.

So far many practical designers and analysts are keen to the lifting line model only for the reason that it easily incorporates airfoil wind tunnel data. This may be done for the lifting surface model also, with theoretically-proven averaging of the chordwise variable inductive washdown. Without deep insight into what "theoretically-proven" is, just note a simple consideration. If lifting surface analysis calculation gives approximately constant washdown in chordwise direction, then both lifting line and lifting surface models are valid. Otherwise means that incorporating of airfoil aerodynamic data into the lifting line model is not correct. This is not important for straight unswept blades of high aspect ratio, however it's strongly important for curved low aspect ratio blades.

2.1 Aerodynamic model. Nonlinearity

An aerodynamic model of a rotor is always nonlinear, as vortex sheet pitch depends on the rotor thrust. Correct determination of vortex sheet pitch is the main factor to obtain the thrust value. All aerodynamic derivatives also depend on the pitch (here we mean derivatives at constant pitch used in aeroelastic stability analysis). That is why flutter performance depend not only on rotation speed, but on pitch as well.

The existing methods to determine the vortex sheet pitch may be divided into two classes:

The first one includes pitch determination on the basis of a simplified (impulse, Zhukovsky's theory e.t.c.), with consequent application of a more precise approach (lifting line or lifting surface).

The second class includes methods of iterative or other type pitch determination on the basis of a unified theoretical model.

We lean towards the first class method, proposing, in our opinion, the best version.

The essence of the method considered is as follows. The inductive velocity is known to be constant over the rotor disk if the spanwise circulation distribution delivers minimum inductive losses at the assigned power supplied to the rotor.

To avoid any misunderstanding, let us define explicitly what the inductive velocity is. Hereafter, the **inductive velocity V_{ind} is the velocity of a uniform flow, which component, normal to the sheet, and at the sheet, is the same, as the normal to the sheet component of the velocity induced by the sheet.** No velocity component is constant downstream the rotor, but for the rotor with minimum inductive losses, the component normal to the sheet, though not constant, is the same as if produced by a uniform flow 'blowing' onto the sheet with the velocity V_{ind}. It's clear that vortex sheet is a constant pitch helical surface in this case.

The numerical algorithm is as follows. At the first step, the vortex sheet pitch is taken from application of Zhukovsky's rotor theory. The spanwise circulation distribution is calculated that delivers minimum inductive losses at the assigned power supplied to the rotor. Inductive velocity V_{ind} is calculated, and pitch value for the next iteration is determined. Stable and efficient iterative procedure has been developed successfully. There is no need to consider blade model, but infinite vortex sheet only, which results in small dimension of the problem.

2.2 Aerodynamic model. Compressibility effect.

It should be noted that the Prandtl-Glauert transformation cannot be used to consider air compressibility as the equation for flow potential has variable coefficients if written in the system of coordinates connected to the blade. Thus an ordinary 4-dimensions wave equation has to be solved for a quasi-steady problem (4th coordinate is time). This problem is solved by the method of "descending along the coordinate (time)". Functions of influence of singularities (sources and vortices) moving along a helical line are used. Noерштп more is needed for vertical blowdown mode.

Sometimes a linear blade analysis is thought to be unreliable if it demonstrates supercritical pressure coefficient on the blade surface. Fortunately, this is not the case. For an airplane

wing, all points of which are moving with the same speed, appearance of local aerodynamic zones is always advertent resulting in shock-induced losses. Vise versa, as the blade points are moving with different speeds and local Mach numbers, no interference between propagating disturbance waves takes place, and thus strong shock waves with entropy loss do no occur.

The above effect reduces the accuracy of transferring airfoil experimental derivatives into lifting line analysis, though the error is on the safe side concerning flutter.

3 ELASTIC AND INERTIAL MODELS.

Both elastic and inertial properties of the blade are set up within NASTRAN-based finite element models (FEM).

In-house mech generator and settings module to set up finite elements properties and materials reology data has been made for NASTRAN. It accelerates data preparation for FE analysis. Once the blade geometry is set up or obtained from aerodynamic optimization module, then all the other is done automatically and faster than by use of PATRAN. Also automated are transferring aerodynamic loads onto FEM of the blade and generation of a matrix of aerodynamic influence coefficients (for static aeroelasticity analysis), matrices of aerodynamic stiffness and aerodynamic damping (for aeroelastic stability analysis).

An automatically generated FEM model may be enlarged and edited then in PATRAN preprocessor. The interface algorithm between in-house and PATRAN preprocessor is designed so that no updating is required.

NASTRAN features the widest capabilities of modeling inertial and elastic configurations, both schematic ones and identical "one-to-one". Any springs and dampers may be introduced; rotor hub flexibility matrix or hinges may be simulated with the aid of superelements; any mechanism may be introduced (e.g., pitch-flap coupling mechanism). Many of these options are available from in-house preprocessor also, and both complement each other.

Also there are a lot of capabilities for composite materials simulation in NASTRAN, and all these are available from the authors' interface. Shell, Solid and Beam elements may be set up, as well as variable shell thickness, vector fields of anisotropy axes for composite materials and their laminate stacks.

3.1 Elastic and inertial models. Nonlinearity.

Nonlinear formulation of elastic and inertial models seems necessary.

Basically, it does not seem necessary for beam-based model, however a FEM model in NASTRAN version does makes it necessary. Unfortunately, we do not know any means to adjust NASTRAN for correct modeling of a fairly linear effect, i.e. centrifugal inertial forces field, without use of nonlinear algorithms.

Nonlinear formulation slightly complicates flutter analysis and makes programs running slower, which is undesirable for CAD/CAE software.

To accelerate program running, a dedicated optimal algorithm has been developed for NASTRAN, which essentially shorten processor time for nonlinear analysis.

It happened possible to provide the interaction with NASTRAN, in which eigenvalues and eigenvectors problem is solved at each intermediate step (rpm increment). As a result, we can built resonance rpm diagram (Campbell's diagram) and get all necessary data on nonlinear elastic/inertial model of the blade for rpm values within the operational range, having consumed the run time only 30% longer than one nonlinear analysis cycle. Indeed, it's possible because the problem of obtaining first dozen or two dozens of vibration modes is solved very fast, e.g. by means of Lanczoc method. It's also intuitively clear how we can built a matrix of aerodynamic influence coefficients at each rpm step.

3.2 Identification of inertial and elastic model of the blade.

The most direct way to get the source data for identification of an elastic system is experimental modal analysis, which in our case should be performed on a rotating blade.

However, this is not too easy and feasible from many points of view.

Meantime, it's possible to develop an "inexpensive" identification procedure of an elastic system well described by the equations of beam bending. The key idea is the refusal from finding bending stiffness of the beam in a set of spanwise stations, but getting its flexibility matrix (structural influence coefficients) instead. An n x n flexibility matrix may be obtained by applying force in each of n reasonably selected structural points and measuring displacements from the applied force in all these points. The techniques is rather consumable for matrix of high dimensions, e.g. when numerous vibration modes have to be obtained. It seems expedient to develop a procedure of getting matrix of any dimensions for any nodes allocation on the basis of a standard procedure and moderate number of measurements. Let's formulate the above in a formal manner:

Definition. The problem of identification of elastic properties of a beam is solved, if a procedure has been developed to obtain n *x* m *flexibility matrix {A} that provide correspondence between any finite set of displacements* $[u_1, \dots, u_n]$ *in points of the beam with any finite set of forces applied in assigned points of the beam* $[f_1, \dots, f_m]$*:*

$$[u]^T = \{A\}[f]^T \qquad (1)$$

Of course, we cannot expect to be able to find out such a procedure with fixed scope of measurements for any beam with an arbitrary spanwise stiffness distribution. It's evident however that a beam with rather a simple stiffness distribution may be identified in the above sense by a small number of measurements, and then it's possible to generate a flexibility matrix of any dimension for any set of nodal points.

Let us consider a beam cantilevered at its left end. Now we demonstrate a useful flexibility matrix properties of the beam by proving a simple *Statement 1*.

Before formulation and proving the Statement, note that we really can limit ourselves with consideration of a left cantilever beam, as to get the flexibility matrix then for the same beam with any other boundary conditions is a trivial mathematical task.

Statement 1. Let $a_{ij} = a(x_i, x_j)$ *be a component of the cantilevered beam matrix, equal, by definition, to the displacement in a point* x_i *under the unit force applied in a point* x_j*. Then, for any fixed* x_i *and any* $x_j > x_i$, *the following relationship takes place*

$$a(x_i,x_j)=C_{1i}+C_{2i}\,x_j, \tag{2}$$

where constants C_{1i}, C_{2i} *do not depend on* x_j.

The proof. Evidently, the beam deflection line from a unit force applied in x_i is a straight line at $x_j>x_i$. In other words

$$a(x_j,x_i)=C_{1i}+C_{2i}\,x_j, \tag{2'}$$

Now we can write down the procedure to build up the flexibility matrix for a left cantilevered beam. Let the beam be placed within segment [0,1] in x coordinate.

As $a(x_j,x_i) = a(x_i,x_j)$ (the rule of reciprocity of the mechanical work), then (2) follows from (2'). *End of proving.*

Not let's write down the procedure to build up the flexibility matrix for a left end cantilevered beam. The beam occupies [0,1] segment in x axis.

- Let's generate Chebyshev's grid within [0,1] so that $X_1=0$, $X_n=1$.

- A Chebyshev's grid is generated within each segment $[0,X_j]$; $j=1, \ldots$, so that:

- $$x_{1j}=0,\ x_{mj}=X_j.$$

- A force is applied subsequently in each point $X_2 , \ldots , X_n$, as well as in the point $X_{n+1}=1.5$ (to apply the force in X_{n+1}, a rigid arm is attached to the right end with moment bearing); displacements in the points $\{x_{2j}, \ldots ,x_{mj}\}U\{ X_2 , \ldots , X_{n+1} \}$ are measured for each force application in the point X_j, $j=2, \ldots , n+1$.

- A set of n-1 twice continuously differentiable interpolants is built on the basis of measured displacements $\{u(x_{2j}), \ldots ,u(x_{mj})\}U\{ u_j(X_j) , \ldots ,u_j(X_{n+1}) \}$

  for $j=2, \ldots$ n;

  each interpolant satisfying the boundary conditions $I_j(0)=0$, $I_j{}'(0)=0$, $I_j{}'(X_j)= [u_j(X_{j+1})-u_j(X_j)]/(X_{j+1}-X_j)$, $I_j{}''(X_j)=0$.

  Also one continuously differentiable interpolant that satisfies the boundary conditions $I_{n+1}(0)=0$, $I_{n+1}{}'(0)=0$, $I_{n+1}{}'(X_n)= [u_{n+1}(X_{n+1}) -u_{n+1}(X_n)]/(X_{n+1}- X_n)$ is built.

  The interpolants $I_{j<n+1}(x)$ are polynomials of m+2 power at $x<X_{j<n+1}$,

  $I_{n+1}(x)$ is an m+1 order polinomial, and all these are the linear functions at $x>X_{j<n+1}$.

- A k x n flexibility matrix {A} may be built for an arbitrary set of nodal points, which displacements are of interest, i.e.:

- $$a(x^*{}_i,X_j)=I_j(x^*{}_i);\ i=1, \ldots ,k;\ j=2, \ldots n+1.$$

- From the matrix just described above, with the use of the results of proving the *Statement 1* (linear interpolation along the matrix line within the upper triangle), and

from the mechanical work reciprocity principle (matrix lower triangle is symmetric to the upper one) a k x k' flexibility matrix may be obtained for a set of nodal points

- $$\{x^*_1, \dots , x^*_k\}U\{x^{**}_1, \dots , x^{**}_{k'}\};$$

where $\{x^{**}_1, \dots , x^{**}_{k'}\}$ – the points of force application.

Of course, the most common is the particular case of the square matrix, when $\{x^*_1, \dots , x^*_k\}$ and $\{x^{**}_1, \dots , x^{**}_{k'}\}$ are the same.

A matrix of slope angles $\{A\}^{'}$ (x-derivative), and a matrix of curvatures $\{A\}^{''}$ (second x-derivative) may be obtained similarly. The difference is that the work reciprocity principle is not easy to use to obtain the lower triangle in this case. From the *Statement 1* it follows that the $\{A\}^{''}$ lower triangle is zero, while the $\{A\}^{'}$ lower triangle includes constants for each column. It can be simply derived that $a'(x_i,x_j) = [a(x_{i''},x_j) - a(x_{i'},x_j)]/(x_{i''} - x_{i'})$ at $x_{i''}, x_{i'} < x_j$.

Below is an example of the beam with linear spanwise stiffness (not flexibility!) variation. Simulated "measured" stiffness values are compared with the exact solution. The comparison show rather acceptable quality of the algorithm. Below, l is the beam length, (curvature is presented as a fracture of l, and a slope angle is presented in %s).

	EI(x)			№		
"Mesured"	0,952			X force		
Exact	0,950	№	X	displacement		
				Slope		
				Curvature		

Table 2: The structure of flexibility matrix

EI(x)	X		1	2	3	4	5	6	
		X	99	278	500	723	902	1001	
0,952	1	99	0,08	0,31	0,58	0,86	1,08	1,21	
0,950			0,1249	0,5796	1,1465	1,7135	2,1681	2,4204	:100
			0	0,0470	0,1055	0,1641	0,2111	0,2372	:I
0,863	2	278	0,31	1,85	4,11	6,36	8,17	9,17	
0,861			0,1249	1,0124	2,6758	4,3391	5,6730	6,4133	:100
			0	0	0,0646	0,1292	0,1811	0,2098	:I
0,747	3	500	0,58	4,11	11,18	18,82	24,95	28,35	
0,750			0,1249	1,0124	3,4310	6,6378	9,2094	10,6365	:100
			0	0	0	0,0746	0,1345	0,1677	:I
0,638	4	723	0,86	6,36	18,82	34,88	48,30	55,74	
0,638			0,1249	1,0124	3,4310	7,5102	11,5244	13,7521	:100
			0	0	0	0	0,0700	0,1089	:I
0,562	5	902	1,08	8,17	24,94777	48,29843	69,65	81,71	
0,549			0,1249	1,0124	3,4310	7,5102	12,1749	15,1445	:100
			0	0	0	0	0	0,0441	:I
	6	1001	1,21	9,17	28,35	55,74	81,71	96,88	
			0,1249	1,0124	3,4310	7,5102	12,1749	0,1537	:100
			0	0	0	0	0	0	:I

Table 3: Flexibility matrix in initial points

EI(x)		X	1 0	2 200	3 400	4 600	5 800	6 1000	
0,995	1	0	0,00	0,00	0,00	0,00	0,00	0,00	
1,000			0,0000	0,0001	0,0002	0,0003	0,0005	0,0006	:100
			0	0,0503	0,1005	0,1508	0,2010	0,2513	:I
0,901	2	200	0,00	0,68	1,72	2,75	3,79	4,82	
0,900			3E-09	0,5174	1,5705	2,6236	3,6767	4,7298	:100
			0	0	0,0555	0,1109	0,1664	0,2219	:I
0,798	3	400	0,00	1,72	5,62	9,92	14,22	18,51	
0,800			3E-09	0,5174	2,1488	4,3779	6,6070	8,8361	:100
			0	0	0	0,0626	0,1253	0,1879	:I
0,695	4	600	0,00	2,75	9,92	19,54	29,61	39,67	
0,700			3E-09	0,5174	2,1488	5,0324	8,6015	12,1706	:100
			0	0	0	0	0,0718	0,1436	:I
0,601	5	800	0,00	3,79	14,21737	29,60745	47,79	66,49	
0,600			3E-09	0,5174	2,1488	5,0324	9,3512	14,4653	:100
			0	0	0	0	0	0,0829	:I
	6	1000	0,00	4,82	18,51	39,67	66,49	96,57	
			3E-09	0,5174	2,1488	5,0324	9,3512	0,1533	:100
			0	0	0	0	0	0	:I

Table 4: Interpolated flexibility matrix

Extended flexibility matrix for the Gauss-Chebyshev quadrature formula

EI(x)		X	13	109	283	500	718	892	988
0,991	1	13	0,00	0,00	0,01	0,01	0,01	0,02	0,02
0,994			0,0021	0,0326	0,0877	0,1564	0,2251	0,2802	0,3108
			0	0,0244	0,0684	0,1233	0,1781	0,2221	0,2466
0,947	2	109	0,00	0,11	0,37	0,70	1,03	1,30	1,45
0,945			0,00206	0,1518	0,6412	1,2515	1,8618	2,3512	2,6228
			0	0	0,0460	0,1034	0,1608	0,2068	0,2324
0,860	3	283	0,01	0,37	1,97	4,26	6,55	8,38	9,40
0,858			0,00206	0,1518	1,0546	2,7115	4,3683	5,6970	6,4344
			0	0	0	0,0632	0,1264	0,1771	0,2052
0,747	4	500	0,01	0,70	4,26	11,18	18,63	24,60	27,92
0,750			0,00206	0,1518	1,0546	3,4310	6,5574	9,0645	10,4558
			0	0	0	0	0,0728	0,1311	0,1635
0,641	5	718	0,01	1,03	6,547088	18,62741	34,05	46,91	54,05
0,641			0,00206	0,1518	1,0546	3,4310	7,3854	11,2609	13,4116
			0	0	0	0	0	0,0680	0,1057
0,566	6	892	0,02	1,30	8,38	24,60	46,91	67,23	78,70
0,554			0,00206	0,1518	1,0546	3,4310	7,3854	0,1188	14,7278
			0	0	0	0	0	0	
	7	988	0,0194	1,445014	9,402826	27,91842	54,05082	78,70231	94,95
			0,00206	0,151793	1,054608	3,431041	7,385443	0,118759	0,1536
			0	0	0	0	0	0	0

Table 4: Extended flexibility matrix for the Gauss-Chebyshev quadrature formula

It would be useful to bring the blade identification problem to a more observable result than just a flexibility matrix. The more common and observable one is Campbell's diagram, which is useful to conclude whether the blade is suitable for flight service. The algorithm to build the Campbell's diagram is also easy to develop. Below is the diagram for the above mentioned blade, as well as vibration mode shapes for the first 4 modes at maximum rpm. The flexibility matrix for the blade model has been built on the basis of 6 nodal points.
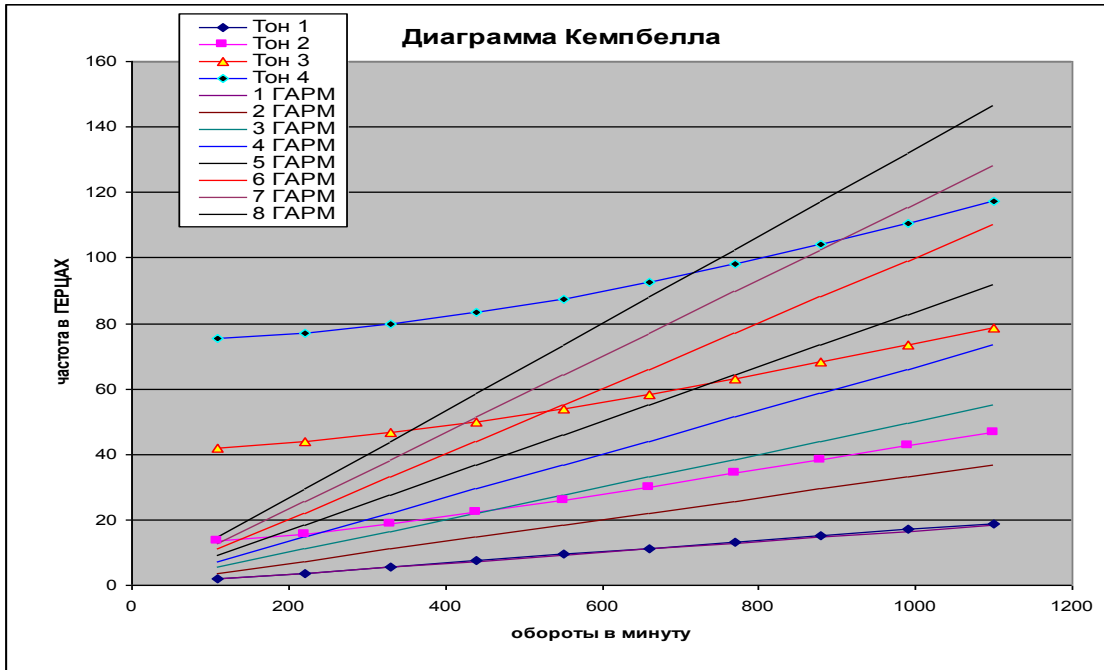
Figure 1: Campbell's diagram
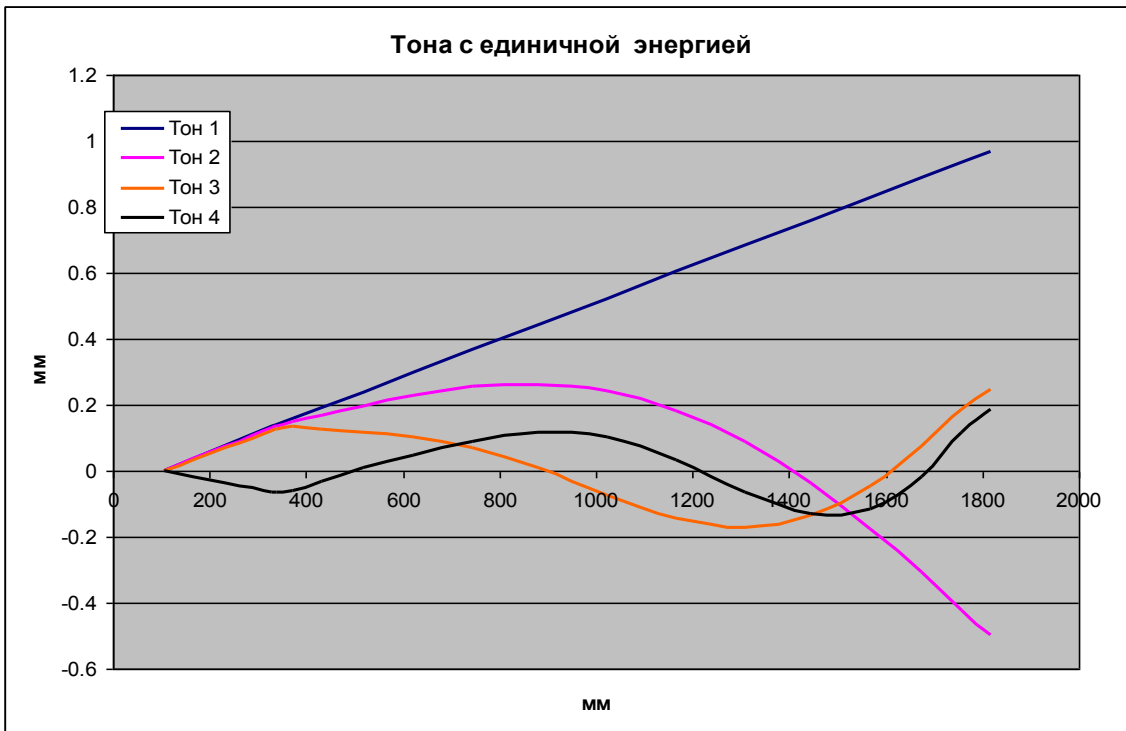
Figure 2: Vibration mode shapes scaled to unit energy

Below is the brief description how the results shown above (Campbell's diagram and mode shapes) can be derived.

Suppose we know almost exactly the beam mass distribution (e.g. by sawing it into pieces and weighing each peace).

So, let mass per unit length spanwise distribution is known:

$$m(r) = P_n(r) \quad r \in [r_0, R] \tag{3}$$

Let the beam is rotating with unit angular velocity. Then:

$$N(r) = \int_r^R m(r')r'dr' \quad \text{is the tension force, which is n+2 order polynomial in this case.}$$

Consider the equation of the beam disturbed motion:

$$\left(EIy''\right)'' - \omega^2 \left(Ny'\right)' + my = 0$$

Let's reduce (by a standard techniques) the system with infinite number of degrees of freedom (DOFs) to the system with finite number of DOFs.

Let

$$y(r) = y_0 \frac{r - r_{\text{ш}}}{r_0 - r_{\text{ш}}} + \sum_{k=1}^m y_k f_k(r)$$

$$f_k(r) = \frac{(r - r_0)^S \prod_{\substack{i=1 \\ i \neq k}}^m (r - r_i)}{(r_k - r_0)^S \prod_{\substack{i=1 \\ i \neq k}}^m (r_k - r_i)} \quad \text{where} \quad r_i, i = 1,...,m \quad nodes \quad of \quad Gauss \quad formula \tag{4}$$

Basis functions $f_k(r)$ are chosen so that $f_k(r_k) = 1$, and $f_k(r_i) = 0$ if $i \neq k$.

If S>1, then $f_k(r_0) = 0$ and $f_k'(r_0) = 0$. The last condition means embedding blade root into the hub cutout.

If 0<S≤1, then only $f_k(r_0) = 0$. The last condition means supporting the blade on the hub cutout.

Real (not integer) S may be used for some specific tasks.

After substitution (12), the equations of the system with finite DOFs system are written as follows:

$$\left(\{A\} + \omega^2 \{B\}\right)y + \{C\}\frac{d^2\mathbf{y}}{dt^2} = 0$$

13

The stiffness matrix {A} for a non-rotating blade has been already determined by means of measurements and some mathematical transformations. So let's write how matrices {B} and {C} look like.

A Gauss quadratic formula is used below to substitute summation for integration. Note, use of quadratic formulas give exact integral value if $2(n+1) < 2m$.

The nomenclature below is as follows:

h_k – weights of the Gauss quadratic formula;

$M_k = m(r_k)h_k$ – «lumped masses»;

N_i ,$f_{ik} = N(r_i),f_k(r_i)$ e.t.c. ;

r_h – radial location of a horizontal hinge;

r_0 – radial location of the blade root section;

I_h – blade moment of inertia about horizontal hinge axis;

I_{axi} – blade moment of inertia about the horizontal axis crossing the rotor axis of rotation;

I_{hh} – the hub cutout moment of inertia of about the horizontal hinge axis;

S_h – static moment of inertia about the horizontal hinge axis;

S_{axi} – the blade static moment of inertia about the horizontal axis crossing the rotor axis of rotation;

S_{hh} – the hub cutout static moment of inertia about the horizontal hinge axis.

The formulas to determine matrix {B}:

$$\left(\mathbf{y},\{B\}\mathbf{y}\right) = -\int_{r_0}^{R} y(Ny')'dr = -\,y(R)N(R)y'(R) + y(r_0)N(r_0)y'(r_0) + \int_{r_0}^{R} Ny'^2 dr =$$

$$y_0^2 N(r_0)/(r_0 - r_h) + \int_{r_0}^{R} N\left[y_0/(r_0 - r_h) + \sum_{k=1}^{m} y_k f_k'(r) \right]^2 dr =$$

$$y_0^2 N(r_0)/(r_0 - r_h) + \int_{r_0}^{R} N\left\{ y_0^2/(r_0 - r_h)^2 + 2y_0 \sum_{k=1}^{m} y_k f_k'(r)/(r_0 - r_r) + \left[\sum_{k=1}^{m} y_k f_k'(r) \right]^2 \right\} dr$$

From these transformations it follows that:

$$b_{00} = N(r_0)/(r_0 - r_{\mathrm{h}}) + \int_{r_0}^{R} N dr /(r_0 - r_{\mathrm{h}})^2 = N(r_0)/(r_0 - r_{\mathrm{h}}) + \sum_{i=1}^{M} N_i h_i /(r_0 - r_{\mathrm{h}})^2$$

<div align="center">or</div>

$$b_{00} = N(r_0)/(r_0 - r_{\mathrm{h}}) + \int_{r_0}^{R} N dr /(r_0 - r_{\mathrm{h}})^2 =$$

$$= N(r_0)/(r_0 - r_{\mathrm{r}}) + \left[N(R)R - N(r_0)r_0 + \int_{r_0}^{R} mr^2 dr \right]/(r_0 - r_{\mathrm{h}})^2 =$$

$$= \left[\int_{r_0}^{R} mr^2 dr - N(r_0)r_0 \right]/(r_0 - r_{\mathrm{h}})^2 = \left[I_{\mathrm{axi}} - S_{\mathrm{axi}} r_0 \right]/(r_0 - r_{\mathrm{h}})^2 =$$

$$= \left[I_{\mathrm{axi}} - Mr_{\mathrm{h}}^2 - \left(S_{\mathrm{axi}} - Mr_{\mathrm{h}} \right)r_0 - Mr_{\mathrm{h}}(r_0 - r_{\mathrm{h}}) \right]/(r_0 - r_{\mathrm{h}})^2 = \left[I_h - Mr_{\mathrm{h}}(r_0 - r_{\mathrm{h}}) - S_{\mathrm{h}} r_{\mathrm{h}} \right]/(r_0 - r_{\mathrm{h}})^2$$

The following should be added to b_{00} to take into account the hub cutout:

$$\int_{r_{\mathrm{ш}}}^{r_0} m_{\mathrm{h}} r(r - r_{\mathrm{h}}) dr /(r_0 - r_{\mathrm{h}})^2 = \frac{I_{\mathrm{hh}} + r_{\mathrm{r}} S_{\mathrm{hh}}}{(r_0 - r_{\mathrm{h}})^2}$$

$$b_{0k} = b_{k0} = \sum_{i=1}^{M} N_i f'_{ik} h_i /(r_0 - r_{\mathrm{h}}) = \int_{r_0}^{R} N f_k' dr /(r_0 - r_{\mathrm{h}}) = \left[N(R)f_k(R) - N(r_0)f_k(r_0) - \int_{r_0}^{R} N' f_k dr \right]/(r_0 - r_{\mathrm{h}}) =$$

$$= \int_{r_0}^{R} m f_k r dr /(r_0 - r_{\mathrm{h}}) = \sum_{i=1}^{M} m_i h_i f_{ik} r_i /(r_0 - r_{\mathrm{h}}) = m_k h_k r_k /(r_0 - r_{\mathrm{h}}) = M_k r_k /(r_0 - r_{\mathrm{h}})$$

$$b_{jk} = b_{kj} = \sum_{i=1}^{M} N_i f'_{ij} f'_{ik} h_i = \int_{r_0}^{R} N f_j' f_k' dr = N(R)f_j'(R)f_k(R) - N(r_0)f_j'(r_0)f_k(r_0) - \int_{r_0}^{R} \left(N f_j' \right)' f_k dr =$$

$$= -\sum_{i=1}^{M} \left(N_i f'_{ij} \right)' f_{ik} h_i = -\left(N_k f'_{kj} \right)' h_k = \left(m_k r_k f'_{kj} - N_k f''_{kj} \right) h_k = M_k r_k f'_{kj} - N_k f''_{kj} h_k$$

The formulas to determine matrix {C}:

$$(\mathbf{y}, \{C\}\mathbf{y}) = \int_{r_0}^{R} y^2 m dr = \int_{r_0}^{R} \left[y_0 (r - r_{\mathrm{h}})/(r_0 - r_{\mathrm{h}}) + \sum_{k=1}^{m} y_k f_k(r) \right]^2 m dr =$$

$$= \int_{r_0}^{R} \left\{ y_0^2 (r - r_{\mathrm{h}})^2 /(r_0 - r_{\mathrm{h}})^2 + 2 y_0 \sum_{k=1}^{m} y_k f_k(r)(r - r_{\mathrm{h}})/(r_0 - r_{\mathrm{h}}) + \left[\sum_{k=1}^{m} y_k f_k(r) \right]^2 \right\} m dr$$

From these transformations it follows that

$$c_{00} = \int_{r_0}^{R} (r - r_{\rm h})^2 \, m dr / (r_0 - r_{\rm h})^2 = I_{\rm hh} / (r_0 - r_{\rm h})^2$$

$$c_{0k} = c_{k0} = \int_{r_0}^{R} (r - r_{\rm h}) f_k(r) m dr / (r_0 - r_{\rm h}) = M_k (r_k - r_{\rm h}) / (r_0 - r_{\rm h})$$

$$c_{kk} = \int_{r_0}^{R} f_k^2(r) m dr = M_k$$

Other components of the matrix are 0.

The value of $\dfrac{I_{\rm hh}}{(r_0 - r_{\rm h})^2}$ should be added to b_{00} to take into account the hub cutout.

Functions $f_k(r)$ and their first and second derivatives have been already used above. Below are some useful formulas for derivatives of basis functions:

Let's note for simplicity

$$\alpha = \frac{1}{(r_k - r_0)^S \displaystyle\prod_{\substack{i=1 \\ i \neq k}}^{m} (r_k - r_i)}$$

The expression for the first derivative:

$$f_k' = \alpha \left((r - r_0)^S \prod_{\substack{i=1 \\ i \neq k}}^{m} (r - r_i) \right)' = \alpha \left[S(r - r_0)^{S-1} \prod_{\substack{i=1 \\ i \neq k}}^{m} (r - r_i) + (r - r_0)^S \prod_{\substack{i=1 \\ i \neq k}}^{m} (r - r_i) \sum_{\substack{i=1 \\ i \neq k}}^{m} \frac{1}{r - r_i} \right] =$$

$$= f_k \left(\frac{S}{r - r_0} + \sum_{\substack{i=1 \\ i \neq k}}^{m} \frac{1}{r - r_i} \right)$$

Let's resolve the uncertainty of 0/0 type:

$$f_k'(r_0) = \theta(1 - S) S \alpha \prod_{\substack{i=1 \\ i \neq k}}^{m} (r_0 - r_i) \tag{1}$$

$$f_k'(r_l) = \frac{(r_l - r_0)^S \displaystyle\prod_{\substack{i=1 \\ i \neq k,l}}^{m} (r_l - r_i)}{(r_k - r_0)^S (r_k - r_l) \displaystyle\prod_{\substack{i=1 \\ i \neq k,l}}^{m} (r_k - r_i)} \quad \Rightarrow \quad f_k'(r_l) f_l'(r_k) = -\frac{1}{(r_k - r_l)^2} \quad \text{if } l \neq k \cup l > 1$$

The expression for the second derivative:

$$f_k'' = \alpha\left(S(r-r_0)^{S-1}\prod_{\substack{i=1\\i\neq k}}^{m}(r-r_i) + (r-r_0)^S\prod_{\substack{i=1\\i\neq k}}^{m}(r-r_i)\sum_{\substack{i=1\\i\neq k}}^{m}\frac{1}{r-r_i}\right)' =$$

$$= \alpha\left\{\begin{array}{l}S(S-1)(r-r_0)^{S-2}\prod_{\substack{i=1\\i\neq k}}^{m}(r-r_i) + 2S(r-r_0)^{S-1}\prod_{\substack{i=1\\i\neq k}}^{m}(r-r_i)\sum_{\substack{i=1\\i\neq k}}^{m}\frac{1}{r-r_i} + \\ + (r-r_0)^S\prod_{\substack{i=1\\i\neq k}}^{m}(r-r_i)\left[\left(\sum_{\substack{i=1\\i\neq k}}^{m}\frac{1}{r-r_i}\right)^2 - \sum_{\substack{i=1\\i\neq k}}^{m}\frac{1}{(r-r_i)^2}\right]\end{array}\right\}$$

или

$$f_k'' = \left[f_k\left(\frac{S}{r-r_0} + \sum_{\substack{i=1\\i\neq k}}^{m}\frac{1}{r-r_i}\right)\right]' = f_k'\left(\frac{S}{r-r_0} + \sum_{\substack{i=1\\i\neq k}}^{m}\frac{1}{r-r_i}\right) - f_k\left(\frac{S}{(r-r_0)^2} + \sum_{\substack{i=1\\i\neq k}}^{m}\frac{1}{(r-r_i)^2}\right)$$

Again let's resolve the uncertainty of 0/0 type:

$$f_k''(r_0) = \alpha S(S-1)\prod_{\substack{i=1\\i\neq k}}^{m}(r_0-r_i) \tag{1}$$

$$f_k''(r_l) = 2\alpha(r_l-r_0)^S\prod_{\substack{i=1\\i\neq k,l}}^{m}(r_l-r_i)\sum_{\substack{j=1\\j\neq k,l}}^{m}\frac{1}{r_l-r_j} = 2f_k'(r_l)\sum_{\substack{j=1\\j\neq k,l}}^{m}\frac{1}{r_l-r_j} \quad if \quad l>0 \cup l\neq k$$

If r equals only r_k, or it does not equal to any $\{r_i\}$, then there are no uncertainties.

4 THE PROBLEM FORMULATION FOR THE OBLIGUE BLOWING OVER THE HELICOPTER MAIN ROTOR

Let's first formulate an aeroelastic problem for the main rotor under vertical blowdown.

Let L be an aerodynamic matrix providing correspondence between intensities of discrete vortices "attached" to the blade with the displacements in the points where aerodynamic boundary conditions are set up (non-permeability condition).

Thus

$$\bar{u} = \frac{\rho}{2}\{L\}\{V\}\overline{\Gamma},$$

where $\{V\}$ is a diagonal matrix of flow velocities in the points of vortices allocation:

Evidently, the matrix L may be built because of linear relationship between discrete vortices intensities and pressure values on the blade surface. The transformation matrix from the pressure values in surface points to the displacements in the points where boundary conditions are set up may be obtained either experimentally (as shown above), or by nonlinear static problem FEM solution.

Note that the solution of the nonlinear static problem for a rotating blade is much more reliable, effective and proven than the problem of determination of mode shapes for rotating blades. The latter would have to be resorted if a dynamic condensation method were used.

The static aeroelasticity problem is formulated then as follows:

$$\{D\}\overline{u} + \overline{\alpha} = \{V'\}^{-1}\{A\}\overline{\Gamma}$$
$$\Downarrow$$
$$\frac{\rho}{2}\{D\}\{L\}\{V\}\overline{\Gamma} + \overline{\alpha} = \{V'\}^{-1}\{A\}\overline{\Gamma} \tag{5}$$

Or in a resolved form:

$$\left\{-\frac{\rho}{2}\{D\}\{L\}\{V\} + \{V'\}^{-1}\{A\}\right\}\overline{\Gamma} = \overline{\alpha} \tag{6}$$

It has been noted above:

$\{D\}$ is a matrix between displacements and slope angles (differentiation matrix);

$\{V'\}$ is a diagonal matrix of velocities in the control points to satisfy boundary conditions;

$\{A\}$ is a matrix of aerodynamic influence setting the correspondence between vorticies intensities and the velocities induced by them in control points.

The above formulation (6) is applicable for the analysis of the main rotor under vertical blowdown. It's checked by many researches, highly effective and allows the HOT COLD GEOMETRY problem to be solved easily.

It may seem strange that when a rotor just starts moving [forward] in the plane of rotation, then such a problem formulation is not used, but a dynamic condensation method is used at once instead. A question arises why a continuous transition is not considered at all!

The answer may be as follows:

For the steady motion of the main rotor, the following should be the periodic functions of time (with the blade rotation period):

non-permeability condition, matrix of aerodynamic influence, and vortices intensities.

Let's build the solution iteratively. First select N uniformly spaced moments in time, within one period of rotation, and get the solution of the static aeroelasticity problem at each moment. Once the moment is fixed, then the problem may be treated as "quasistatic".

$$\left\{-\frac{\rho}{2}\{D\}\{L\}\{V(t_k)\} + \{V'(t_k)\}^{-1}\{A(t_k)\}\right\}\{\Gamma(t_k)\} = \{\alpha(t_k)\}; \quad k = 1,...,N \qquad (7)$$

If the number of blades is n, and they are supplied with horizontal hinges, then the matrix of solutions and the right hand side have n+1 columns each.

The first column of the right hand side contains non-permeability conditions corresponding to an assigned law of the cyclic pitch variation; the kth column contains non-permeability conditions corresponding to unit angular velocity of the kth blade flap motion with all other blades motionless. From the columns of the matrix of solutions corresponding to such right hand sides, we can get one column by calculating n values of flap angular velocity from the n equations of zero moment in the horizontal hinge. The matrix of such a system is almost diagonal due to the slight cross-influence between the blades.

For the moment bearing attachment of the blade root, only the first column is enough, and the solution is got at once.

Now perform the next iteration. The idea of iterations is to correct the right hands side at each next step by adding non-permeability conditions caused by inertial unloading and the velocities that are the mismatches between "quasistatic" and dynamic solutions.

To obtain velocities and accelerations, let's write the displacements

$$\bar{u}_0(t_k) = \frac{\rho}{2}\{L\}\{V(t_k)\}\bar{\Gamma}_0(t_k) \quad k = 1,...,N$$

in the form of Fourier series:

$$\bar{u}(t) = \sum_{s=0}^{\left[\frac{N}{2}\right]}\bar{a}_s \cos \omega st + \bar{b}_s \sin \omega st \qquad (8)$$

Then

$$\dot{\bar{u}}(t_k) = \omega \sum_{s=1}^{\left[\frac{N}{2}\right]} s\left(\bar{b}_s \cos \omega st_k - \bar{a}_s \sin \omega st_k\right)$$

$$\ddot{\bar{u}}(t_k) = -\omega^2 \sum_{s=1}^{\left[\frac{N}{2}\right]} s^2\left(\bar{a}_s \cos \omega st_k + \bar{b}_s \sin \omega st_k\right)$$

By adding, to the first column of the right-hand side (7), the non-permeability conditions

$$\bar{\alpha}_{\text{inertion}}(t_k) = \{D\}\{L\}\{M\}\ddot{\bar{u}}(t_k)$$

from the deformation due to inertial unloading,

and non-permeability conditions from the velocities

$$\overline{\alpha}_{\text{dumping}}(t_k) = \{V'\}^{-1}\overline{\overline{u}}(t_k),$$

we get the solution of equations (7),

find out flap angular velocity for each blade,

get one column of solutions for circulations and displacement at each time moment,

represent the displacements as Fourier series,

calculate non-permeability conditions from inertial unloading,

calculate non-permeability conditions from the velocity,

e.t.c.

4 CONCLUSIONS

The authors regard the above consideration as promising and propose it for futher implementation in design practice

5 REFERENCES

[1]   Bisplinghoff R., Ashley H., Halfman R., Aeroelasticity, Addison-Wesley Publishing Company, Inc., Cambridge 42, Mass., 1955

6 COPYRIGHT STATEMENTS